

NITROGEN ADSORPTION ON DOUBLE-WALLED CARBON NANOTUBE AT DIFFERENT TEMPERATURES: MECHANISTIC INSIGHTS FROM MOLECULAR DYNAMICS SIMULATIONS

 Utkir B. Uljayev*, Shakhnozaxon A. Muminova,  Ishmumin D. Yadgarov

Arifov Institute of Ion-Plasma and Laser Technologies, Academy of Sciences of Uzbekistan, Tashkent, 100125, Uzbekistan

**Corresponding Author e-mail: utkir.uljaev@outlook.com*

Received December 22, 2023; revised January 12, 2024; accepted January 24, 2024

Nitrogen-adsorbing carbon nanotubes have received considerable attention in the field of materials science due to their unique properties and potential applications. In particular, nitrogen-adsorbed double-walled carbon nanotubes (DWNTs) can exhibit a wide range of tunable electronic and optoelectronic properties. In this study, the effect of different temperatures (i.e., 300, 600, and 900 K) of DWNT on nitrogen adsorption is investigated through molecular dynamics simulations using the ReaxFF potential. The simulation results show a good nitrogen storage capacity of DWNT, particularly at 600 K, reaching a maximum gravimetric density of 12.4 wt%. This study contributes to a better understanding of the mechanisms governing nitrogen adsorption onto DWNTs at different temperatures.

Keywords: *Double-walled carbon nanotube, Nitrogen adsorption, Reactive molecular dynamics*

PACS: 61.46.-w, 02.70.Ns

INTRODUCTION

Carbon nanotubes (CNTs) have garnered broad interest across physics, chemistry, and materials science [1], showcasing promise in diverse applications including electronic devices [2], sensors [3], material reinforcement [4], adsorbents [5], and numerous other areas [7]. Among them, double-walled carbon nanotubes (DWNTs) have gained significant attention due to their improved stability and mechanical properties [8],[9]. The interactions of DWNTs with other atoms and molecules, particularly boron (B) [10], nitrogen (N) [11], calcium (Ca) [12], palladium (Pd) [13] and platinum (Pt) [14] have been intensively studied in recent years.

Among them, nitrogen (N) atoms adsorption (i.e., chemisorption) on carbon nanotubes has gained much attention in recent years due to its applications in various fields such as energy storage and catalysis [5], [6]. N atom chemisorption and doping on DWNTs are being explored as promising strategies to modify their electrical and chemical properties for various applications. Several studies have investigated the chemisorption mechanism of N atoms on the outer and inner walls of DWNTs, as well as the effect of N doping on their electronic and optical properties [15]. Chemisorption of N atoms on DWNTs depends on various factors, such as tube diameter and chirality, which in turn affect the strength and type of interaction with the adsorbate [11]. In this respect, understanding the chemisorption processes of N atoms on DWNTs is essential for the design of efficient nanomaterials for gas detection and separation [16], [17], [18]. Although nitrogen (N) atoms have been introduced into CNTs by various methods (e.g., CVD, ALD), controlling their amount in the structure is still one of the pressing problems [19], [20].

In this study, we investigate the chemisorption mechanisms of N atoms on DWNT at different temperatures using molecular dynamics (MD) simulations.

COMPUTATIONAL DETAILS

The process of nitrogen adsorption onto DWNTs is investigated using reactive MD simulations [21] using the LAMMPS package [22]. The ReaxFF potential is used to describe the interatomic interactions in the system [23]. This potential is chosen to describe the breaking and joining of bonds between atoms. A neat (5,5@10,10) nanotube was chosen as a DWNT model (DWNT(5,5)@(10,10)) in MD simulations (Fig.1). The diameter of DWNTs is 6.78 and 13.57 Å (Fig. 1) which is in the range of experimentally obtained nanotube diameters (6.3 Å–7.9 Å) and (13 Å–16 Å) [24]. Periodic boundary conditions are applied along the z-axis, which represents the length of the DWNT (28.12 Å), allowing the simulation of infinitely long DWNTs.

Initially, the energy of all model systems is minimized by the conjugated gradient method. Subsequently, the temperature and pressure of the systems are equilibrated to the desired values (300 K, 600, 900K and 0 Pa) in the NpT ensemble using a Berendsen thermostat and barostat [25] with coupling constants of 100 fs and 5000 fs, respectively. The chosen heating rate (i.e., 1 K/ps) corresponds to a previously reported range of values (0.1–10.0 K/ps) [26] and indicates that the deviations in the thermodynamic equilibrium of the model systems are insignificant during the temperature increase. In the case of the chemisorption of N atoms on DWNT, the system's temperature is kept at 300 K, 600 K and 900 K for 100 ps using a Bussi thermostat [27] with a coupling constant of 100 fs in the canonical NVT ensemble.

In the simulations, the pressure of N atoms in the system is calculated as $p = J\sqrt{2\pi MRT}/N_A$, [28] (1), where J is the impingement flux ($\text{nm}^{-2}\cdot\text{ns}^{-1}$), N_A is Avagadro's number, R is the universal gas constant, M is the molar mass of the N atom ($\text{kg}\cdot\text{mol}^{-1}$) and T is the temperature of the system (K). In this work, the impingement flux of the incident N atoms (i.e., 100 N) is $78.74 \text{ nm}^{-2}\cdot\text{ns}^{-1}$, and its corresponding pressure is approximately 1.94 MPa. The simulation is done under NVT conditions with N atoms added to the environment surrounding the surface of the nanotube at a 10 ps interval, and with a minimum distance of 10 Å (i.e., the cutoff radius of the interaction potential) between each N atoms and the model system.

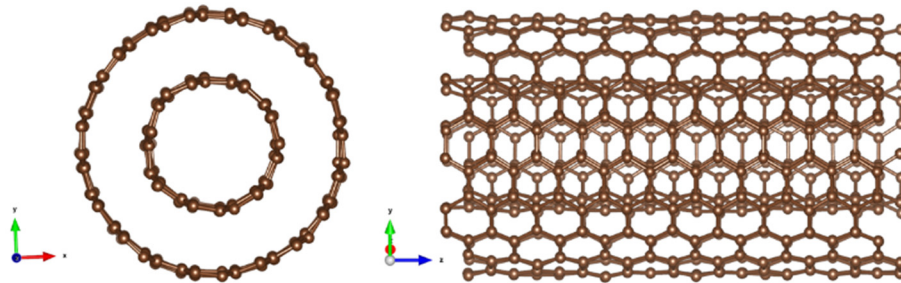


Figure 1. Top and side views of the DWNT(5,5)@(10,10) model system

The gravimetric density of nitrogen (N) atoms remaining on the surface of pure DWNTs under the influence of different temperatures (300 K, 600 K, 900 k) was calculated as follows:

$$wt\% = (1 + m_C N / m_N n)^{-1} \times 100\% \quad (1)$$

where m_C and N are the mass and number of carbon atoms in DWNT, m_N and n are the mass and number of adsorbed N atoms.

In all MD simulations, a time step of 0.1 fs is used. The simulations are repeated 5 times for each study case, and the final results are obtained by averaging the individual physical quantities.

RESULTS AND DISCUSSION

It can be seen from the results that N atoms adsorbed on the DWNT(5,5)@(10,10) surface for systems with different temperatures (i.e. 300, 600, 900 K) number adsorption N (%) atoms (or adsorption index, $(N_{\text{adsorption}}/N_{\text{total}}, \%)$) also varied. Specifically, with an increase in the number of adsorbed N atoms at a temperature of 300 K, the number of adsorbed N atoms was in the range of 2-48% (Fig.2a). Temperature of 600 K and 900 K, it is in the range of 2-77% and 10-61%, respectively.

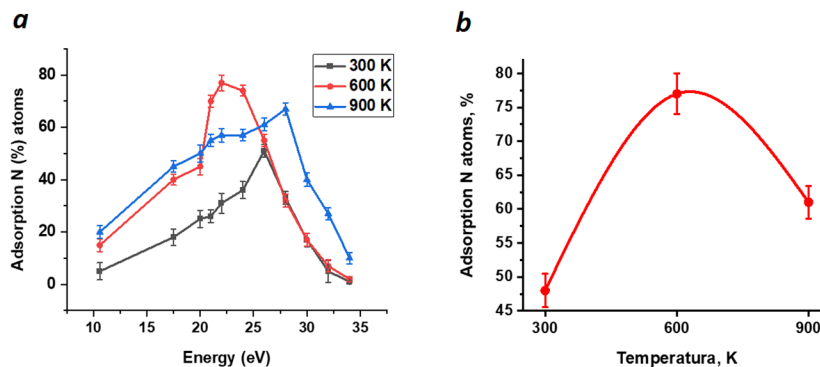


Figure 2. (a) Dependence of the number of adsorbed nitrogen (N) atoms on their kinetic energy, (b) The temperature dependence of the maximum adsorption index of nitrogen atoms.

That is, at temperatures of 300 K, 600 K and 900 K, the maximum adsorption index was equal to 48%, 77% and 61% (Fig.2b). The largest adsorption index is at 600 K, which is 1.52 and 1.19 times greater than at 300 K and 900 K. It can be seen from the results that the adsorption index did not increase linearly with increasing temperature. From the results, it is known that the temperature also affects the N adsorption process. As the velocity (i.e., kinetic energy) of N atoms falling on the DWNT(5,5)@(10,10) surface increased, the adsorption level also increased (from 0 eV to 22.50 eV), further increasing the velocity of N atoms led to a decrease in the amount of adsorption (about, 26.24 eV for 300 K, 22.50 eV for 600 K and 28.74 eV for 900 K). The results indicate that an additional elevation in energy (i.e., 33.15 eV) led to a decrease in the adsorption index to a value approaching 0% (Fig.2a).

The chemisorption of N atoms on DWNT relies on multiple factors, such as the curvature of the nanotube surface, the arrangement of the six-membered carbon rings, among others [29],[30]. Furthermore, the adsorption index of DWNT varies at different temperatures. Depending on their position (para, ortho, meta) within the hexagon cell of the CNT,

N atoms on the surface of CNT can depart from the surface due to the influence of temperature [31]. N atoms adsorbed on the DWNT surface are influenced by the arrival of other N atoms on the surface, leading to the formation of molecules through the Langmuir-Hinshelwood recombination mechanism (where two N atoms on the surface covalently bond to form a nitrogen molecule) or Eley-Rideal desorption mechanism on the surface due to the impact of incoming N atoms on the adsorbed N atom [32], [33]. The temperature range (i.e., 300–900 K) employed in this study altered the quantity of N atoms adsorbed on the surface.

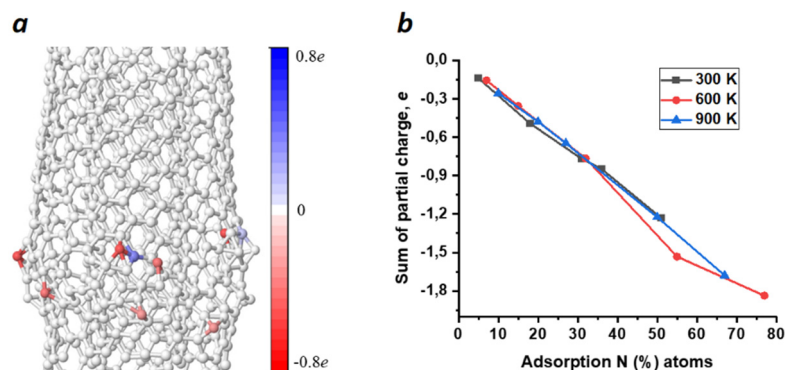


Figure 3. (a) N atoms chemisorbed onto DWNT(5,5)@(10,10) are introduced, and system atoms exhibit partial charges from $-0.8e$ to $+0.8e$, which range from red to blue is depicted by the color spectrum, which shows the transition from electron-rich regions to electron-poor regions, respectively, (b) The alteration in the partial charge of adsorbed N atoms in relation to temperature

In addition to these effects, in CNT, the carbon atom has a higher electronegativity value ($\chi=2.55$) compared to the N atom ($\chi=3.04$). Figure 3a shows the chemisorption process of N atoms on DWNT(5,5)@(10,10). Atoms in the system are depicted in blue with a positive charge and red with a negative charge, while uncharged (0) atoms are depicted in white. This difference in electronegativity results in interactions such as Coulomb forces between the CNT surface and N atoms. This, in turn, results in a relatively stronger interaction between N atoms and C atoms on the DWNT(5,5)@(10,10) surface, thereby leading to higher adsorption of N atoms on DWNT(5,5)@(10,10). Figure 3b illustrates that the partial charge increases with the rise in the adsorption index (%) of chemisorbed N atoms on DWNT(5,5)@(10,10).

Table 1. The variation in the partial charge of adsorbed nitrogen (N) atoms (%) is demonstrated as a function of temperature.

Adsorption N atoms, %	300 K		Adsorption N atoms, %	600 K		Adsorption N atoms, %	900 K	
	C	N		C	N		C	N
5	$0.14e$	$-0.14e$	7	$0.15e$	$-0.15e$	10	$0.25e$	$-0.25e$
18	$0.49e$	$-0.49e$	15	$0.35e$	$-0.35e$	20	$0.48e$	$-0.48e$
31	$0.76e$	$-0.76e$	32	$0.76e$	$-0.76e$	27	$0.65e$	$-0.65e$
36	$0.85e$	$-0.85e$	55	$1.53e$	$-1.53e$	50	$1.22e$	$-1.22e$
51	$1.23e$	$-1.23e$	77	$1.84e$	$-1.84e$	67	$1.67e$	$-1.67e$

As a result, the sum of maximum partial charges of C and N atoms appropriately $1.23e$ and $-1.23e$ (51 %) for 300 K, $1.84e$ and $-1.84e$ (77 %) for 600 K, $1.67e$ and $-1.67e$ (67 %) for 900 K which corresponds to the values of 5–77 % respectively (Table 1). This indicates that an increase in the concentration of N leads to an increase in negative (n-type) partial charges of the DWNT. This validates the outcomes achieved in earlier investigations [34].

Figure 4 shows the nitrogen adsorption coverage ($\rho\%=N_N/N_C$) and gravimetric density (wt%) of N atoms as a function of temperature. As can be seen from the figure, the ρ % (or, wt%) of N atoms at 300, 600 and 900 K is different, the maximum adsorption of N atoms on the surface at 300 K, 600 K and 900 K level 8 % (or 9.3 wt%), 12.1 % (or 12.4 wt%), 10.18% (or 10.6 wt%), respectively.

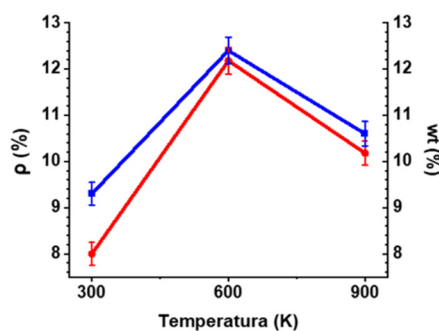


Figure 4. The gravimetric density of chemisorbed N atoms (right, blue) and the adsorption coverage (left, red) as a function of temperature

CONCLUSION

We can conclude that this molecular dynamics simulation has successfully visualized the N adsorption mechanism in DWNT(5,5)@(10,10). In this simulation the trend of N adsorbed in DWNT(5,5)@(10,10) is influenced by temperature factors. The N adsorption by DWNT(5,5)@(10,10) at lower temperatures such as at 300 K has a higher amount of N concentration than at higher temperatures (600 K and 900 K). As the temperature increases at a constant pressure, the amount of N that adsorbed will be decreases. While the trend of the amount of N absorbed will growth with increasing pressure at a constant temperature. The best result of gravimetric density 12.4 wt% (or 12.1% nitrogen concentration) that occurred at 1.94 MPa pressure with temperature (600 K) condition.

Acknowledgment

This research was carried out within the framework of the F-FA-2021-512 project, granted by the Agency for Innovative Development of the Republic of Uzbekistan. The simulations were performed using FISTUz cluster at the Institute of Ion-Plasma and Laser Technologies of the Academy of Sciences of Uzbekistan.

ORCID

©Ishmumin D. Yadgarov, <https://orcid.org/0000-0002-4808-2258>; ©Utkir B. Uljayev, <https://orcid.org/0009-0002-2564-5270>

REFERENCES

- [1] S. Iijima, "Carbon nanotubes: past, present, and future", *Phys. B Condens. Matter*, **323**(1-4), 1–5 (2002). [https://doi.org/10.1016/S0921-4526\(02\)00869-4](https://doi.org/10.1016/S0921-4526(02)00869-4)
- [2] M. Soto, et al., "Effect of interwall interaction on the electronic structure of double-walled carbon nanotubes", *Nanotechnology*, **26**(16), 165201 (2015). <https://doi.org/10.1088/0957-4484/26/16/165201>
- [3] Q. Wei, X. Tong, G. Zhang, J. Qiao, Q. Gong, and S. Sun, "Nitrogen-Doped Carbon Nanotube and Graphene Materials for Oxygen Reduction Reactions", *Catalysts*, **5**(3), 1574–1602 (2015). <https://doi.org/10.3390/catal5031574>
- [4] E.N. Nxumalo, and N.J. Coville, "Nitrogen Doped Carbon Nanotubes from Organometallic Compounds: A Review", *Materials*, **3**(3), 2141–2171 (2010). <https://doi.org/10.3390/ma3032141>
- [5] F. Shojaie, "N₂ adsorption on the inside and outside the single-walled carbon nanotubes by density functional theory study", *Pramana*, **90**(1), 4 (2018). <https://doi.org/10.1007/s12043-017-1498-5>
- [6] M. Jamshidi, M. Razmara, B. Nikfar, and M. Amiri, "First principles study of a heavily nitrogen-doped (10,0) carbon nanotube", *Phys. E Low-Dimens. Syst. Nanostructures*, **103**, 201–207 (2018). <https://doi.org/10.1016/j.physe.2018.06.003>
- [7] C. Zhao, Y. Lu, H. Liu, and L. Chen, "First-principles computational investigation of nitrogen-doped carbon nanotubes as anode materials for lithium-ion and potassium-ion batteries", *RSC Adv.* **9**(30), 17299–17307 (2019). <https://doi.org/10.1039/C9RA03235E>
- [8] S.-P. Ju, et al., "A molecular dynamics study of the mechanical properties of a double-walled carbon nanocoil", *Comput. Mater. Sci.* **82**, 92-99 (2014). <https://doi.org/10.1016/j.commatsci.2013.09.024>
- [9] V. Zólyomi, et al., "Intershell interaction in double walled carbon nanotubes: Charge transfer and orbital mixing", *Phys. Rev. B*, **77**(24), 245403 (2008). <https://doi.org/10.1103/PhysRevB.77.245403>
- [10] T. Koretsune, and S. Saito, "Electronic structures and three-dimensional effects of boron-doped carbon nanotubes", *Sci. Technol. Adv. Mater.* **9**(4), 044203 (2008). <https://doi.org/10.1088/1468-6996/9/4/044203>
- [11] K.-Y. Chun, H.S. Lee, and C.J. Lee, "Nitrogen doping effects on the structure behavior and the field emission performance of double-walled carbon nanotubes", *Carbon*, **47**(1), 169–177 (2009). <https://doi.org/10.1016/j.carbon.2008.09.047>
- [12] S.H. De Paoli Lacerda, J. Semberova, K. Holada, O. Simakova, S. Hudson, and J. Simak, "Carbon Nanotubes Activate Store-Operated Calcium Entry in Human Blood Platelets", *ACS Nano*, **5**(7), 5808–5813 (2011). <https://doi.org/10.1021/nn2015369>
- [13] H. Wu, D. Wexler, and H. Liu, "Effects of different palladium content loading on the hydrogen storage capacity of double-walled carbon nanotubes", *Int. J. Hydrog. Energy*, **37**(7), 5686–5690 (2012). <https://doi.org/10.1016/j.ijhydene.2011.12.120>
- [14] D. Xia et al., "Extracting the inner wall from nested double-walled carbon nanotube by platinum nanowire: molecular dynamics simulations", *RSC Adv.* **7**(63), 39480–39489 (2017). <https://doi.org/10.1039/C7RA07066G>
- [15] J.D. Correa, E. Florez, and M.E. Mora-Ramos, "Ab initio study of hydrogen chemisorption in nitrogen-doped carbon nanotubes", *Phys. Chem. Chem. Phys.* **18**(36), 25663–25670 (2016). <https://doi.org/10.1039/C6CP04531F>
- [16] H. Soleymanabadi, and J. Kakemam, "A DFT study of H₂ adsorption on functionalized carbon nanotubes", *Phys. E Low-Dimens. Syst. Nanostructures*, **54**, 115–117 (2013). <https://doi.org/10.1016/j.physe.2013.06.015>
- [17] R. Kronberg, H. Lappalainen, and K. Laasonen, "Hydrogen Adsorption on Defective Nitrogen-Doped Carbon Nanotubes Explained via Machine Learning Augmented DFT Calculations and Game-Theoretic Feature Attributions", *J. Phys. Chem. C*, **125**(29), 15918–15933 (2021). <https://doi.org/10.1021/acs.jpcc.1c03858>
- [18] Y. Fujimoto, and S. Saito, "Structure and stability of hydrogen atom adsorbed on nitrogen-doped carbon nanotubes", *J. Phys. Conf. Ser.* **302**, 012006 (2011). <https://doi.org/10.1088/1742-6596/302/1/012006>
- [19] M. Terrones, A. Jorio, M. Endo, A.M. Rao, Y.A. Kim, T. Hayashi, H. Terrones, et al., "New direction in nanotube science", *Mater. Today*, **7**(10), 30–45 (2004). [https://doi.org/10.1016/S1369-7021\(04\)00447-X](https://doi.org/10.1016/S1369-7021(04)00447-X)
- [20] M. Glerup, M. Castignolles, M. Holzinger, G. Hug, A. Loiseau, and P. Bernier, "Synthesis of highly nitrogen-doped multi-walled carbon nanotubes", *Chem. Commun.* **20**, 2542 (2003). <https://doi.org/10.1039/b303793b>
- [21] B.J. Alder, and T.E. Wainwright, "Phase Transition for a Hard Sphere System", *J. Chem. Phys.* **27**(5), 1208–1209 (1957). <https://doi.org/10.1063/1.1743957>
- [22] A.P. Thompson, H.M. Aktulga, R. Berger, D.S. Bolintineanu, W.M. Brown, P.S. Crozier, P.J. Veld, et al., "LAMMPS - a flexible simulation tool for particle-based materials modeling at the atomic, meso, and continuum scales", *Comput. Phys. Commun.* **271**, 108171 (2022). <https://doi.org/10.1016/j.cpc.2021.108171>
- [23] K. Chenoweth, A. C. T. Van Duin, and W. A. Goddard, "ReaxFF Reactive Force Field for Molecular Dynamics Simulations of Hydrocarbon Oxidation", *J. Phys. Chem. A*, vol. 112, no. 5, pp. 1040–1053, 2008, <https://doi.org/10.1021/jp709896w>

- [24] G. Chen, *et al.*, “Chemically Doped Double-Walled Carbon Nanotubes: Cylindrical Molecular Capacitors”, *Phys. Rev. Lett.* **90**(25), 257403 (2003). <https://doi.org/10.1103/PhysRevLett.90.257403>
- [25] H.J.C. Berendsen, J.P.M. Postma, W.F. Van Gunsteren, A. DiNola, and J.R. Haak, “Molecular dynamics with coupling to an external bath”, *J. Chem. Phys.* **81**(8), 3684–3690 (1984). <https://doi.org/10.1063/1.448118>
- [26] J. Sun, P. Liu, M. Wang, and J. Liu, “Molecular Dynamics Simulations of Melting Iron Nanoparticles with/without Defects Using a Reaxff Reactive Force Field”, *Sci. Rep.* **10**(1), 3408 (2020). <https://doi.org/10.1038/s41598-020-60416-5>
- [27] G. Bussi, D. Donadio, and M. Parrinello, “Canonical sampling through velocity rescaling”, *J. Chem. Phys.* **126**(1), 014101 (2007). <https://doi.org/10.1063/1.2408420>
- [28] D. Ugarte, A. Châtelain, and W.A. De Heer, “Nanocapillarity and Chemistry in Carbon Nanotubes”, *Science*, **274**(5294), 1897–1899 (1996). <https://doi.org/10.1126/science.274.5294.1897>
- [29] P. Ayala, A. Grüneis, T. Gemming, D. Grimm, C. Kramberger, M.H. Rummeli, F.L. Freire Jr., *et al.*, “Tailoring N-Doped Single and Double Wall Carbon Nanotubes from a Nondiluted Carbon/Nitrogen Feedstock”, *J. Phys. Chem. C*, **111**(7), 2879–2884 (2007). <https://doi.org/10.1021/jp0658288>
- [30] W. Su, X. Li, L. Li, D. Yang, F. Wang, X. Wei, W. Zhou, *et al.*, “Chirality-dependent electrical transport properties of carbon nanotubes obtained by experimental measurement”, *Nat. Commun.* **14**(1), 1672 (2023). <https://doi.org/10.1038/s41467-023-37443-7>
- [31] U. Khalilov, A. Bogaerts, B. Xu, T. Kato, T. Kaneko, and E. C. Neyts, “How the alignment of adsorbed ortho H pairs determines the onset of selective carbon nanotube etching”, *Nanoscale*, **9**(4), 1653–1661 (2017). <https://doi.org/10.1039/C6NR08005G>
- [32] X. Sha, B. Jackson, and D. Lemoine, “Quantum studies of Eley–Rideal reactions between H atoms on a graphite surface”, *J. Chem. Phys.* **116**(16), 7158–7169 (2002). <https://doi.org/10.1063/1.1463399>
- [33] T. Zecho, A. Güttler, X. Sha, D. Lemoine, B. Jackson, and J. Küppers, “Abstraction of D chemisorbed on graphite (0001) with gaseous H atoms”, *Chem. Phys. Lett.* **366**(1-2), 188–195 (2002). [https://doi.org/10.1016/S0009-2614\(02\)01573-7](https://doi.org/10.1016/S0009-2614(02)01573-7)
- [34] R. Czerw, M. Terrones, J.-C. Charlier, X. Blase, B. Foley, R. Kamalakaran, N. Grobert, *et al.*, “Identification of Electron Donor States in N-Doped Carbon Nanotubes”, *Nano Lett.* **1**(9), 457–460 (2001). <https://doi.org/10.1021/nl015549q>

АДСОРБЦІЯ АЗОТУ НА ДВОСТІННИХ ВУГЛЕЦЕВИХ НАНОТРУБКАХ ПРИ РІЗНИХ ТЕМПЕРАТУРАХ: МЕХАНІСТИЧНІ ДОСЛІДЖЕННЯ З МОДЕЛЮВАННЯ МОЛЕКУЛЯРНОЇ ДИНАМІКИ

Уткір Б. Уляєв, Шахнозаксон А. Мумінова, Ішмумін Д. Ядгаров

Інститут іонно-плазмових і лазерних технологій імені Арифова, Академії наук Узбекистану, Ташкент, 100125, Узбекистан
Вуглецеві нанотрубки, що адсорбують азот, привернули значну увагу в галузі матеріалознавства завдяки своїм унікальним властивостям і можливому застосуванню. Зокрема, адсорбовані азотом подвійні стінкові вуглецеві нанотрубки (DWNTs) можуть демонструвати широкий спектр регульованих електронних і оптоелектронних властивостей. У статті досліджується вплив різних температур (300, 600 і 900 K) DWNT на адсорбцію азоту за допомогою моделювання молекулярної динаміки з використанням потенціалу ReaxFF. Результати моделювання показують хорошу здатність DWNT зберігати азот, особливо при 600 K, досягаючи максимальної вагової щільності 12,4% мас. Це дослідження сприяє кращому розумінню механізмів адсорбції азоту на DWNT при різних температурах.

Ключові слова: двостінна вуглецева нанотрубка; адсорбція азоту; реактивна молекулярна динаміка